International Conference on
Plasma Surface Interactions

Cover Page: Fill out and attach to your manuscript.

Paper Number (P-#.#, O-#.#, ---) :	Poster P3-51
Title:	Re-Construction of Detached Divertor Plasma Conditions in DIII-D Using Spectroscopic and Probe Data
Corresponding Authorís Name:	P.C. Stangeby
Affiliation:	University of Toronto Institute for Aerospace Studies
Full Postal Address:	c/o General Atomics P.O. Box 85608 San Diego, California 92186-5608
Telephone #:	(858) 455-4518
Fax#:	(858) 455-4156
E-mail address:	stangeby@fusion.gat.com
Presenting Author (if different from the corresponding author):	
Telephone #:	
Fax #:	
E-mail address:	
Keywords (<7 words):	
PACS numbers (<5)	52.55, 52.20.H, 52.65
JNM subject keywords (<6)	Monte Carlo modeling, Plasma materials interaction, Plasma properties
PSI-16 subject keywords (<6)	DIII-D, Divertor Modeling, OSM, EIRENE
Length in print (*as calculated by form*):	5 journal pages

P3-51

Re-construction of detached divertor plasma conditions in DIII-D using spectroscopic and probe data

S. Lisgo[a], P.C. Stangeby[a], J.D. Elder[a], B.D. Bray[b], N.H. Brooks[b], M.E. Fenstermacher[c], M. Groth[c], D. Reiter[d], J.G. Watkins[e], W.P. West[b], and D.G. Whyte[f]

[a]*University of Toronto Institute for Aerospace Studies, Toronto, M3H 5T6, Canada.*

[b]*General Atomics, San Diego, California 92186-5608, USA.*

[c]*Lawrence Livermore National Laborabory, Livermore, California 94550, USA*

[d]*Forschungszentrum, Juelich*

[e]*Sandia National Laboratories, Albuquerque, New Mexico 87185-1129, USA*

[f]*University of Wisconsin, Madison, Wisconsin 53706, USA.*

Abstract

For some divertor aspects, such as detached plasmas or the private flux zone, it is not clear that the controlling physics has been fully identified. This is a particular concern when the details of the plasma are likely to be important in modeling the problem —for example, modeling co-deposition in detached inner divertors. An empirical method of "reconstructing" the plasma based on direct experimental measurements may be useful in such situations. It is shown that a detached plasma in the outer divertor leg of DIII-D can be reconstructed reasonably well using spectroscopic and probe data as input to a simple onion-skin model and the Monte Carlo hydrogenic code, EIRENE. The calculated 2D distributions of n_e and T_e in the detached divertor were compared with direct measurements from the divertor Thomson scattering system, a diagnostic capability unique to DIII-D.

JNM keywords: Monte Carlo Modeling, Plasma Materials Interaction, Plasma Properties

PSI-16 keywords: DIII-D, Divertor Modeling, OSM, EIRENE

PACS: 52.55, 52.20.H, 52.65

* *Corresponding author address: P.C. Stangeby, c/o General Atomics, P.O. Box 85608, San Diego, California 92186-5608, USA*

* *Corresponding author e-mail: stangeby@fusion.gat.com*

Presenting author address: P.C. Stangeby, c/o General Atomics, P.O. Box 85608, San Diego, California 92186-5608, USA

Presenting author e-mail: stangeby@fusion.gat.com

I. Introduction

Interpretive codes such as TRANSP provide a useful method for analyzing the plasma inside the separatrix by taking experimental radial profiles of n_e, $T_{e,i}$, etc. as input, and extracting information such as $\chi_\perp(r)$ through evaluation of radial particle, momentum and energy balances. It would be valuable to have an equivalent interpretive analysis method for the region outside the separatrix. Such an empirical "re-construction" of the edge plasma could be used to extract cross-field transport information, as for the main plasma. It could also be used to help unravel the complicated atomic physics processes that are always important in the edge: the "background plasma" could be employed as input to the powerful Monte Carlo (MC) neutral hydrogen codes, such as EIRENE, and MC impurity codes such as DIVIMP.

Unfortunately, it will probably be a long time before the exact analogue of TRANSP will be achievable for the edge: (a) the edge region is 2D–3D instead of 1-1/2D, and (b) the spatial coverage of edge diagnostics is typically rather limited. In the meantime, however, a mixed approach can be used to achieve an empirical re-construction of the background plasma, where simple 1D "onion-skin" models/prescriptions [1] are used along with the direct specification of the plasma from experimental data (as much as possible) in order to generate 2D "fields" of the edge plasma quantities, n_e, $T_{e,i}$, $v_{\|}$, etc. The versatile MC codes can then be applied to this background plasma to produce comparisons with additional edge experimental data, such as spectroscopic line emissivities and line shapes, neutral pressure gauge readings, etc. — constituting further constraints on the plasma re-construction.

DIII-D's divertor Thomson scattering (DTS) system [2] provides a unique opportunity to directly measure n_e and T_e in a divertor plasma, even for strongly detached plasma conditions. When combined with magnetic sweeping of the X-point, 2D fields of n_e and T_e are produced over substantial regions of the divertor. DTS data are particularly valuable for empirical plasma re-construction. Unfortunately, on most tokamaks DTS is not available and even on

DIII-D, DTS access to the (generally detached) inner leg is very limited. Since the inner leg is the key region for some of the most critical edge processes — for example, the co-deposition trapping of tritium [3] — there is a strong incentive to develop a method for empirically reconstructing detached divertor plasmas in the absence of DTS. In contrast with DTS, Langmuir probe (measuring I_{sat}^{+}) and spectroscopic measurements are usually available.

The objective of this paper is to establish the basic methodology of empirically reconstructing a detached *outer* leg in DIII-D *using only Langmuir probe and spectroscopic data (no DTS)*. The measure of success is the level of agreement between the reconstructed plasma and the DTS data.

II. Experiment

Low power L-mode [Simple-as-possible plasma (SAPP)] conditions were used with $\bar{n}_e$ = 4.4×10^{19} m^{-3} where the outer divertor leg was weakly detached (shots 105516–9). These SAPP shots are from the same set of experiments as the low density (attached) shots (105500–9), where $\bar{n}_e$ = 2.5×10^{19} m^{-3}, that were analyzed in Ref. [4]. Please see that paper for further details of these shots and of the DIII-D edge diagnostic set that was available.

Two different versions of the Onion-skin method Eirene Divimp edGE (OEDGE) code [1,4] were used in these studies. In the earlier attached-plasma SAPP study of simple (L-mode) attached divertor plasmas, an OSM model that solves the standard fluid conservation equations (particles, momentum, energy) was successfully applied. However, for other divertor operational modes and regions — such as detached plasmas or the private flux zone (PFZ) — it appears that the controlling physics has only been partly identified. This is a particular concern when the details of the plasma are likely to be important in modeling a problem — as appears, for example, to be the situation when trying to model co-deposition in detached inner divertors [1]. In this case, it is appropriate to use a more empirical OSM

version that attempts to reconstruct the plasma from the available experimental data. An example of the application of this approach to the C-Mod PFZ can be found in Ref. [5]. We undertake the same type of analysis here, using the high density SAPP data set — which appears to be the most extensive such set assembled for these simple detached conditions, on any tokamak, and thus provides the best opportunity available to test this method.

III. Empirical Reconstructive Modeling of the Detached Plasma

The Onion-Skin Modeling (OSM) section of OEDGE contains a number of different OSM models and prescriptions. The one used here is called SOL28 and its features are shown in the schematic, Fig. 1. The starting point is to establish the $T(s_{||})$ profile for each individual flux tube in the scrape-off layer (SOL), which is done partly by direct prescription from experiental data, and partly by simple modeling. Next, with the $T(s_{||})$ now available as input, the standard 1D particle and momentum conservation equations are solved for $n_e(s_{||})$, $v_{||}(s_{||})$, etc. for each flux tube. The limited data on T_i is from HeII CER temperature just outside the separatrix, near outside midplane, and it shows $T_e \sim T_i$. In the absence of any other T_i data, $T_e = T_i$ was assumed for all locations. S_u is the upstream location where the upstream T_e (T_u) and n_e (n_u) are specified from experiment — the main Thomson and reciprocating probe for each flux tube. S_{rs} is the *s*tart of the "radiation zone", which can be estimated, e.g. from the CIII "cloud" in the toroidal view camera picture, or from 2D bolometric reconstructions; it turned out that the solution was insensitive to S_{rs}, and so it was put at the X-point for simplicity. S_{re} is the *e*nd of the "radiation zone", which is assumed to occur where T_e has dropped to 5 eV. The location of S_{re} could be assigned as for S_{rs} but here it was assigned from the D_γ toroidal camera view. For detached conditions the D_γ emission is strongly influenced by recombination and the D_γ "cloud" is assumed to extend upward from the target to S_{re}, where $T_e \sim 5$ eV. The peak of the D_γ emission is taken to define S_c, where T_e has dropped so low that parallel heat *c*onvection then carries the remaining power and T_e stays constant at

value T_t to the *t*arget, at S_t. Between S_c and S_{re}, T_e was just smoothly connected from the T_t value to the 5 eV value.

A simple model is applied to the "radiation region" between S_{rs} and S_{re}: the power flux density entering each flux tube is calculated from the standard 2 Point Model relation, $q_{\|} = 2\kappa_o T_u^{7/2}/7L$, where L is the flux tube length.It is assumed that 90% of $q_{\|}$ is radiated uniformly in $s_{\|} \in [S_{rs}, S_{re}]$ and that parallel heat transport is purely conductive.

The ionization source, S_{ion}, is specified to be rectangular in spatial shape, centered at S_{re}, and of total strength equal to the ionic sink rate to the target for each flux tube — taken from the target Langmuir probe I_{sat}^{+} value. The DIII-D SAPP data set included shots for three densities, $\overline{n}_e \approx 2.5,3.5,4.4\times10^{19}$ m^{-3}. The I_{sat}^{+} values were ~ same for the two higher densities, indicating that the highest density plasma (analysed here) was in the "roll over" condition, just entering detachment. Volume recombination is neglected in this initial treatment given the mild level of detachment. All other particle sources/sinks — such as cross-field transport and drifts — have also been ignored. The applied momentum loss term, S_{mom}, was also rectangular in shape, extends from S_{re} to the target, with its magnitude assigned for each flux tube on the basis of the measured pressure ratio, upstream/target.

The target temperature was assigned by a search process: with the foregoing prescription and assuming some value for T_t typical of detached conditions, say 1 eV, the 2D plasma can be solved for, and then EIRENE applied to the resulting "plasma background". It turns out that the D_α, D_β, D_γ emissivitity for detached plasmas is a very sensitive T_e thermometer, making it possible to establish the value of T_t with some accuracy.

Figure 2(a,b) shows T_{eu} and n_{eu}. The Thomson and (midplane) reciprocating profiles were of the same shape but were shifted relative to each other — evidently due to uncertainties in the separatrix location (a known problem for the Thomson in particular). The lines shown in Fig. 2 are the average of the Thomson and probe profiles. Figure 2(d) gives the Langmuir

probe I_{sat}^{+} profile across the outer target. The upstream and target (total) pressures are shown in Fig. 2(c). The target pressure requires that a value of T_{et}, which was set based on comparisons with experimental D_α, D_β, D_γ emission across the target that were obtained from the absolutely calibrated filerscopes and multichord divertor spectrometer, Fig. 3. Different values for T_{et} were assumed as input to the OSM and EIRENE then calculated the emissivities (integrated along the appropriate lines of sight, top inset, Fig. 3), lines in Fig. 3. As can be seen, these hydrogenic lines are very sensitive indicators of T_e for detached conditions, establishing that T_{et} = 0.7–0.9 eV. In this first simple analysis, T_{et} was taken to be constant across the target.

This then completes the required input to constrain the OSM model used here. The code-calculated $n_e(s_{||})$ and $T_e(s_{||})$ profiles for each of the computational "rings" for which there were DTS data are shown in Fig. 4 as lines, with the DTS data shown as points. Ring No. 14 is adjacent to the separatrix and ring 21 is furthest out. The agreement is generally to within the scatter of the data. It is therefore concluded that this first test has been successful and justifies proceeding to further improvements. The latter will include use of toroidally-viewing camera data in D_α light, the use of 2D bolometric reconstructions to identify the radiative-loss region, assignment of individual S_c, S_{rs}, and S_{re} values for each flux tube (here the same values were assigned to every flux tube), evaluation of T_{et} for individual flux tubes, inclusion of volume recombination (calculated by EIRENE) iteratively in the plasma solver.

IV. Conclusions

It has been shown that a moderately detached plasma can be "reconstructed" fairly well using spectroscopic and probe data (target and upstream) to constrain a simple detachment model (momentum loss and $T_e < 5$ eV convection region near the target). The method has been tested by comparing the plasma solution with direct measurements from DIII-D's unique divertor Thomson scattering system. The 2D spatial distributions of the plasma conditions in

detached divertor plasmas can thus be generated even when DTS data are not available – assuming the available probe and spectroscopic data set is similar to the one employed here – and can then be used with Monte-Carlo codes to model processes such as carbon-tritium co-deposition.

Acknowledgments

This research was supported by the U.S. DOE under DE-FC02-04ER54698, W-7405-ENG-48, DE-AC04-94AL85000, DE-FG03-96ER54373, and by a Collaborative Research Opportunities Grant from the Natural Sciences and Engineering Research Council of Canada.

References

[1] T.N. Carlstrom, *et al.,* Rev. Sci. Instrum. **63** (1992) 4901; *ibid* **66** (1995) 493.

[2] J.P. Coad, *et al.,* J. Nucl. Mater. **290-293** (2001) 224.

[3] P.C. Stangeby, *et al.,* J. Nucl. Mater. **313-316** (2003) 883.

[4] P.C. Stangeby, *The Plasma Boundary of Magnetic Fusion Devices*, Institute of Physics Publishing, Bristol (2002).

[5] S. Lisgo, *et al.,* this conference.

Figure Captions

Fig. 1. Schematic of the empirical modeling method used here to reconstruct the plasma in the detached outer divertor of DIII-D. "s" denotes the distance along the field line, with s=0 at the target.

Fig. 2. The upstream T_{eu} (a) and n_{eu} (b) obtained by averaging the data from the (midplane) reciprocating Langmuir probe (+) and the (main) Thomson scattering system (■). The upstream and target (total) plasma pressure assuming 1 eV at the target, (c), assuming $p_e = p_i$. The I_{sat}^{+} profile across the outer target measured by the built-in Langmuir probes, (d). The vertical dashed libes indicate the region of the outer SOL for which DTS data is available.

Fig. 3. The line-of-sight profiles across the outer target of absolutely calibrated D_α, D_β, D_γ emission. Measuremenst (points) from the filterscopes and multichord divertor spectrometer. EIRENE code (lines) assuming different values for T_e at the target. It is thus established that T_{et} = 0.7–0.9 eV.

Fig. 4. OSM-calculated $n_e(s_{||})$ and $T_e(s_{||})$ profiles (lines) for each of the "rings" in the computational grid, for which there were DTS data (points). Ring 14 (Ψ_n = 1.0015) is closest to separatrix and increasing Ψ_n indicates rings further out, toward wall (Ref. [2]). Ψ_n is the normalized flux radial coordinate.

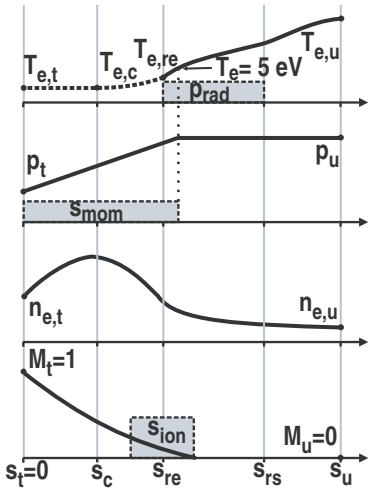

P.C. Stangeby Figure 1

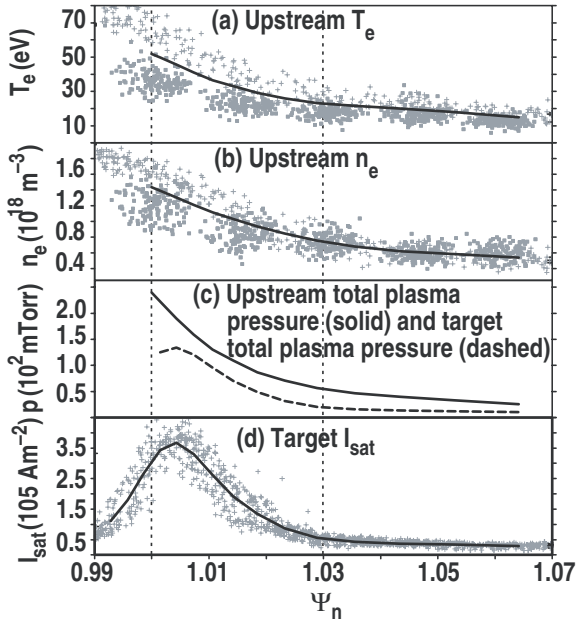

P.C. Stangeby Figure 2

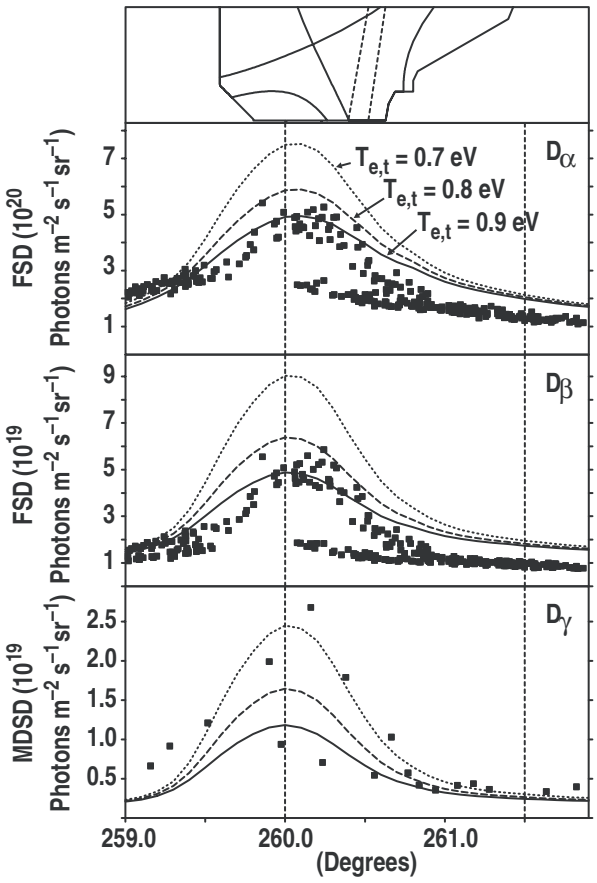

P.C. Stangeby Figure 3

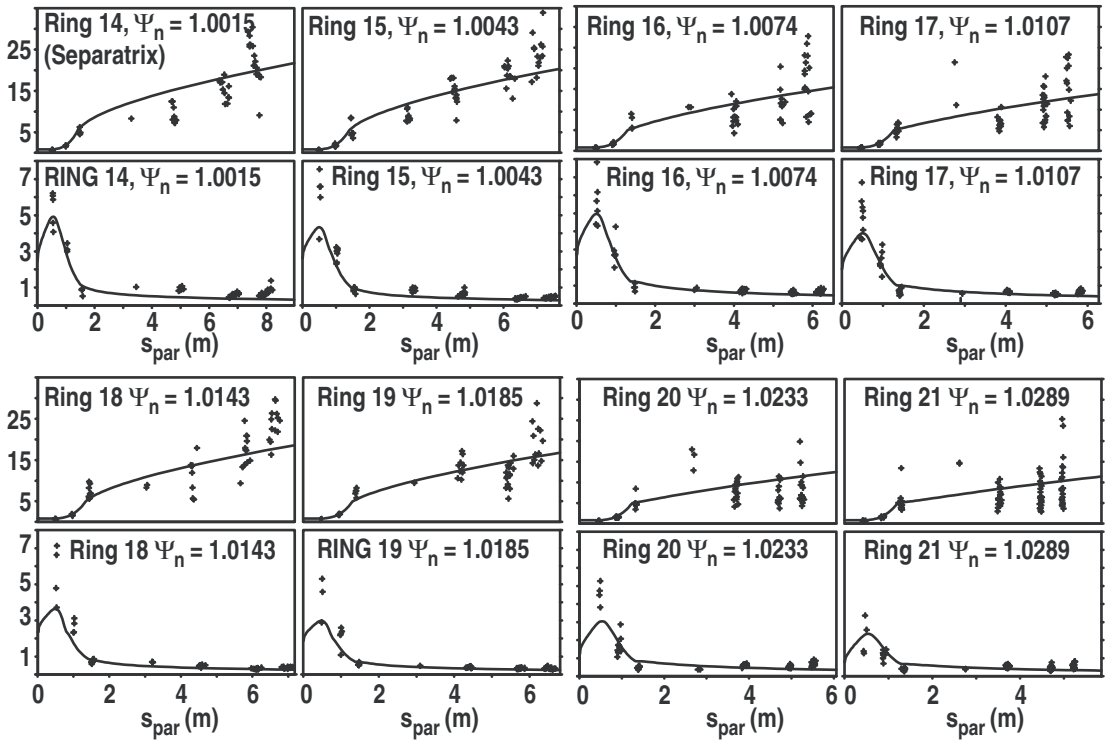

P.C. Stangeby Figure 4

Paper number P3-51

PSI-16 Paper Length Calculation

The length of the manuscript is computed in terms of the number of single-column journal width lines.
All calculations and/or numbers inside brackets (**[xxx]**) are to be rounded up to the next full integer
Limits: 487 lines (oral/poster); 694 lines (invited/long oral); 795 lines (Review)
We strongly advised you to adhere to these limits. The paper may not be accepted for the refereeing process if too long.

			[round up]		
1) Title					
number of characters (including spaces) in title	99	**[x6/58] =**	11		
number of characters (including spaces) in author list	152	**[x4/81] =**	8		
number of affiliations	6	x2 =	12		
Blank lines required by journal added to above			17		
Total lines In Title section			**sum title lines**		48
2) Abstract: A maximum of 150 words is allowed.					
words in abstract	138	**[x1/10] =**	14		
Blank lines required by journal added to above			18		
Total lines In Abstract section			**sum abstract lines**		32
3) Body: Account for words in the body text and spaces between sections and sub-sections.					
number of words in body text	1809	**[x1/9] =**	201		
number of sections (include acknowledgements)	6	x4 =	24		
number of sub-sections	0	x2 =	0		
Total lines In Body section			**sum body lines**		225
4) Figures: All figures should be scaled to either 75 (1 column) or 160 mm (2 column) width.					
Total height (in mm) of 75 mm wide figures	217.5	**[x 0.26] =**	57		
number of words in 75 mm wide figure captions	156	**[x1/8] =**	20		
number of 75 mm wide figures	3	x2 =	6		
Total height (in mm) of 160 mm wide figures	137.5	**[x 0.52] =**	72		
number words in 160 mm wide figure captions	49	**[x1/9] =**	6		
number of 160 mm wide figures	1	x4 =	4		
Total ines In Figures + captions			**sum figure lines**		165
5) Tables					
number of lines (including headings) in 75 mm wide tables	0	x1 =	0		
number of words in 75 mm wide table captions & footnotes	0	**[x1/8] =**	0		
number of 75 mm wide tables	0	x3 =	0		
number of lines (including headings) in 160 mm wide tables	0	x2 =	0		
number of words in 160 mm wide table captions and footnotes	0	**[x1/9] =**	0		
number of 160 mm wide tables	0	x6 =	0		
Total lines In Tables + captions			**sum table lines**		0
6) Equations					
number of characters in 75 mm wide equations	0	**[x 1/40] x 3 =**	0		
number of 75 mm wide equations	0	x2 =	0		
number of characters in 160 mm wide equations	0	**[x 1/100] x 6 =**	0		
number of 160 mm wide equations	0	x4 =	0		
Total lines In Equations			**sum equation lines**		0
7) References					
Lines in references	6	**[x2.16] =**			13
8) Journal space for contact information					**11**
9) Total number of lines from steps 1-8					494